Direct measurement of temperature-dependent solvation forces between DNA double helices

Donald C. Rau and V. Adrian Parsegian
Laboratory of Biochemistry and Metabolism, National Institute of Diabetes and Digestive and Kidney Diseases; and Physical Sciences Laboratory, Division of Computer Research and Technology, National Institutes of Health, Bethesda, Maryland 20892

ABSTRACT The assembly of double stranded DNA helices with divalent manganese ion is favored by increasing temperature. Direct force measurements, obtained from the osmotic stress technique coupled with x-ray diffraction, show that the force characteristics of spontaneously precipitated Mn^{2+}-DNA closely resemble those observed previously by us for other counterion condensed DNA assemblies. At temperatures below the critical one for spontaneous assembly, we have quantitated the changes in entropy and manganese ion binding associated with the transition from repulsive to attractive interactions between helices mediated by osmotic stress. The release of structured water surrounding the DNA helix to the bulk solution is the most probable source of increased entropy after assembly. Increasing the water entropy of the bulk solution by changing the manganese salt anion from Cl^- to ClO_4^- predictably and quantitatively increases the transition entropy. This is further evidence for the dominating role of water in the close interaction of polar surfaces.

INTRODUCTION

The organizing power of ordered water solvent released from the vicinity of the molecular surface has been the cardinal principle of the "hydrophobic" forces so popular in theories of macromolecular organization. Polar surfaces can order water far more strongly and with far more structural detail than can the nonpolar surfaces typically associated with these forces. Indeed, we have been observing for some time now that the mutual structuring of water between two hydrophilic surfaces dominates interaction at close separations. These 'hydration' forces can be either strongly repulsive or strongly attractive depending on the symmetry of water structuring on apposing surfaces. Attractive hydration forces are accompanied by the release of this water into the bulk. It is often forgotten that the free energy of solvent release depends on a *difference* between the values of solvent entropy and enthalpy near the molecular surface and the values far away in the bathing medium.

Through direct measurement of forces between DNA double helices condensed into ordered arrays in various ionic solutions, we have uncovered the existence of attractive hydration forces, one to two orders of magnitude stronger than van der Waals attraction, controlled by the adsorption of specific ions, and extending through several layers of water solvent. We now report a temperature sensitivity of these attractive forces under ionic conditions that minimize the contribution from binding additional ions from solution. Assembly is favored at increased temperature. These attractive hydration forces are predictably strengthened by increasing the entropy of water in the bathing medium, an increase effected by replacing chloride with more "chaotropic" perchlorate ions. This quantitatively verified response to changes in the entropy of the medium indicates the importance of solvent release as the underlying mechanism of DNA assembly into arrays of parallel molecules.

Hydration forces, long known to dominate the interaction of macromolecules or membranes approaching contact, now provide a new way to think about molecular attraction. These forces change with the specific kind of ion bound to the macromolecular surface and even with base pair composition. There is thus a strength, specificity, and control inherent to these interactions previously unrecognized in the attraction of large molecules.

MATERIALS AND METHODS

Chemicals and DNA

All salts were of least analytical grade quality. Manganese chloride tetrahydrate and manganese perchlorate hexahydrate were specifically the highest purity available from Aldrich Chemical Co. (Milwaukee, WI). Polyethylene glycol (PEG), 8,000 average molecular weight, was purchased from Sigma Chemical Co. (St. Louis, MO) and typically used without further purification. Some experiments were done with PEG dialyzed against distilled water and lyophilized to dryness, to ensure that the measurements were not affected by any possible small contaminants in the PEG.

High molecular weight chicken erythrocyte DNA was prepared from whole adult chicken blood (Truslow Farms, Chestertown, MD) as described in McGhee et al. (1981). High molecular weight calf thymus, *Clostridium perfringens*, and *Micrococcus lysodeikticus* DNAs were obtained from Sigma Chemical Co. All were further purified with three extractions against phenol/chloroform (50:50) and once with chloroform alone. The DNA was then ethanol precipitated in Na acetate, pelleted by centrifugation, washed twice with 70% ethanol,

and lyophilized. After dissolving in 10 mM trisCl (pH 7.5), 1 mM EDTA (10-1 TE) at a concentration of ~1 mg/ml, all DNAs were exhaustively dialyzed against 10-1 TE.

Osmotic stress measurements

The method for direct force measurements by osmotic stress has been discussed in detail elsewhere (Parsegian et al., 1986; Rand, 1981; Rau and Parsegian, 1984). Very briefly, DNA pellets (~250 μg) are prepared by precipitation with either ethanol or 5% PEG in appropriate salt solutions. These pellets are equilibrated against PEG-salt solutions in vast excess at known osmotic pressure, ion activities, and temperature. PEG is excluded from the DNA phase and exerts an osmotic pressure on it, whereas water and small ions are free to equilibrate between the two phases. Pellets are typically equilibrated for weeks with several changes of the bathing PEG-salt solution.

The dependence of PEG osmotic pressures on weight concentration and temperature are taken from Michel (1983) (also see Parsegian et al., 1986). We have verified these pressures extensively at 20–25°C. We have not systematically measured temperature dependent PEG osmotic pressures, but those we have measured are in good agreement with the published results. We have additionally verified that the osmotic pressure of a 20% PEG (8,000 MW) solution in 25 mM $MnCl_2$ measured with a Wescor Inc. vapor pressure osmometer (model 5100C; Logan, UT) is, to within ~10%, simply the sum of the separately measured osmotic pressures of 20% PEG in water and of 25 mM $MnCl_2$ with no PEG. There does not seem to be a significant dependence of ion activity on PEG.

X-ray measurements

An Enraf-Nonius Service Corp. (Bohemia, NY) fixed anode Diffractis 601 x-ray generator was used to determine interaxial separations between DNA helices under known osmotic stress. The camera design is described in Mudd et al. (1987). Sample cells contain both the DNA pellet and ~100 μl of the bathing PEG-salt solution. Temperature is regulated by a Peltier heat exchanging device (Cambion model 801-3958-01; see Mudd et al. [1987]) and maintains constant temperature to within ±0.2°C (Mudd et al., 1987). X-ray reflections were detected by film (DEF-5, Eastman-Kodak Co., Rochester, NY). The very strong interaxial reflections were measured either by hand or by scanning densitometer (Podgornik et al., 1989) to give Bragg spacings. Powdered *p*-bromobenzoic acid was used to calibrate sample to film distances (~15 cm). Occasionally, DNA pellets were exposed long enough to confirm hexagonal packing of helices and to observe the 3.4 Å reflection characteristic of B-form DNA. The actual interaxial spacing between helices, D_{int}, for hexagonal packing is related to the Bragg spacing by,

$$D_{int} = 2D_{Br}/\sqrt{3}. \quad (1)$$

Interaxial reflections are sharp and well defined, reproducible to about ±0.2 Å for spacings < 30 Å. Most pellets give powder ring patterns, although it is not unusual for a sample to show a strongly oriented scattering pattern. Spacings >30–35 Å are more diffuse (Podgornik et al., 1989) and reproducible only to within 0.5 Å.

The measured spacings reflect reversible thermodynamic equilibria. A sample equilibrated against one set of osmotic pressure, salt concentration, and temperature conditions can be reequilibrated against another set with no apparent hysteresis or dependence on the initial state of the pellet.

RESULTS

Mn-DNA forces show a transition between repulsion and attraction

Depending on salt conditions, two quite distinct kinds of intermolecular force curves are observed between DNA double helices at close separation by the osmotic stress technique coupled with x-ray diffraction. Both are illustrated in Fig. 1. With all univalent counterions and most divalents (force data in 0.5 M NaCl is shown in the figure), an exponentially increasing repulsive force, independent of ionic strength with a characteristic decay length of ~3 Å (Rau et al., 1984; Podgornik et al., 1987) is seen at close separation (D_{int} < 30–35 Å). Force magnitudes, but not decay length, are dependent on the particular counterion species present, but not on its concentration. The close similarity between this force and that observed between neutral lipid bilayers in distilled water (Rand and Parsegian, 1989), and since then also seen between uncharged carbohydrates helices (Rau and Parsegian, 1990), led us to conclude that repulsive hydration forces due to symmetric water structuring on apposing surfaces dominate the close interaction of DNA helices. At larger distances, salt concentration dependent forces are observed that we have

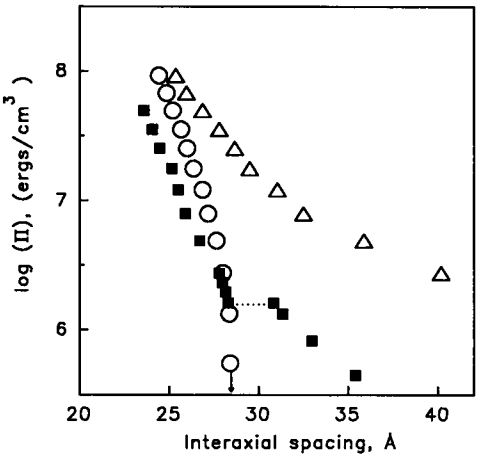

FIGURE 1 Comparison of DNA force curves under different ionic conditions at 20°C. 0.5 M NaCl, 10 mM Tris, 1 mM EDTA (△). 5 mM $Co(NH_3)_6Cl_3$, 0.1 M NaCl, 10 mM Tris (○). 50 mM $MnCl_2$, 10 mM Tris (■). The dependence of the interhelical spacing on the PEG-applied osmotic pressure directly gives intermolecular force curves. The plots show the two kinds of forces we observe between helices, the 3 Å decay length exponentially growing force (at spacings <30–35 Å) seen in 0.5 M NaCl solution and the 1.5 Å decay length exponential characteristic of spontaneously assembled DNA, with $Co(NH_3)_6^{3+}$ for example. The arrow indicates equilibrium spacing of cobalt-precipitated DNA in the absence of applied osmotic stress. The $MnCl_2$ data shows a clear transition from one kind of force to the other.

identified as fluctuation enhanced electrostatic repulsion (Podgornik et al., 1987; Podgornik and Parsegian, 1990).

If sufficient trivalent (or higher charge) counterion concentration is present, DNA helices will spontaneously assemble into an ordered array with a stable 8–12 Å separation between surfaces (or 28–32 Å spacing between helix centers), depending on the particular counterion causing precipitation. There is a balance between repulsive and attractive forces. The measured repulsive force encountered in pushing helices closer than this equilibrium separation increases exponentially with an ~1.3–1.5 Å decay length, or about half the 3 Å length (Rau and Parsegian, 1992), independent of the particular multivalent counterion. A DNA force curve in 5 mM $Co(NH_3)_6Cl_3$ and 0.1 M NaCl, shown in Fig. 1, illustrates this behavior. We have shown that both the force characteristics of the repulsion at close distances and the attraction and can be easily accommodated within the hydration force framework. If two surfaces have both apposing areas of symmetrically structured water (repulsion) and areas of bound water with a complementary structure (attraction) and if the strength of the attraction is greater than the repulsion, then an energy minimum at a finite spacing is predicted and the repulsive force at closer spacings is the second order term of the basic 3 Å decay length exponential, or a 1.5 Å decay exponential.

Included in Fig. 1 is the force behavior observed in 50 mM $MnCl_2$. At low osmotic pressures ($\log \Pi < 6.2$), the force strongly resembles that found in NaCl solution (decay length $\lambda \approx 3.5$ Å). Helices repel at all distances; 50 mM $MnCl_2$ does not cause spontaneous assembly at room temperature. At a certain critical pressure ($\log \Pi = 6.2$), there is a sudden, abrupt decrease in spacing, after which the force characteristics are much more like the $Co(NH_3)_6^{3+}$ curve ($\lambda = 1.4 \pm 0.1$ Å). The curve in 50 mM $MnCl_2$ is closely analogous to the forces observed in salt solution with insufficient cobalt for spontaneous assembly (Rau and Parsegian, 1992).

Precipitation of DNA by Mn with increased temperature

Unlike what is seen for DNA in cobalt hexammine, there is no concentration of $MnCl_2$ that will cause DNA precipitation at room temperature without added osmotic pressure. We do observe, however, that B-form double helical DNA warmed in $MnCl_2$ solutions will visibly "cloud" and eventually form DNA fibers. Clouding temperatures decrease with increasing $MnCl_2$ concentration but never fall below ~40°C (Table 1) even with 0.5 M $MnCl_2$. The visible clouding of the solution is readily reversible upon cooling for transition temperatures less than about 50°C. Knoll et al. (1988) have quantitated this effect for a number of divalent counterions using light scattering, a far more sensitive monitor of assembly than visible clouding, and have reported that precipitation by Mn^{2+} is only slowly reversible under similar conditions.

TABLE 1 Precipitation temperatures from "cloud points"

[Mn]	$Mn(ClO_4)_2$	$MnCl_2$	$MnSO_4$
mM	(°C)	(°C)	(°C)
150	<5	40–45	60–65
50	30–35	40–45	60–65
25	48–53	50–55	65–70
10	68–72	68–72	70–75
5	75–80	75–80	>80

Precipitation is typically reversible if the transition temperature is below ~50°C.

Examining the precipitate by x-ray scattering reveals a hexagonal lattice of parallel molecules with an interaxial spacing ~28 Å, appreciably greater than the molecular diameter of some 20 Å. Apparently, the forces of attraction causing this temperature driven assembly extend well beyond the perimeter of the double helix.

Among the divalent cations we have tested, only Mn^{2+} and Cd^{2+} appear to confer this kind of condensation of double helices at temperatures below about 60°C; Mg^{2+}, Ca^{2+}, Ni^{2+}, Zn^{2+}, and putrescine are all quite powerless in this regard. Divalent Cu^{2+} does precipitate DNA at millimolar concentrations but with no apparent x-ray order in the pellet. DNA denaturation is known to occur at fairly low concentrations of Cu^{2+} (Eichhorn and Shin, 1968).

The action of Mn^{2+} also increases with the GC content of the DNA. The clouding temperature in 50 mM $MnCl_2$ is ~47°C for Clostridium perfringens DNA (26% GC) and ~35°C for *Micrococcus lysodeikticus* DNA (76% GC) compared with ~42°C for chicken erythrocyte and calf thymus DNAs (42 and 43% GC). This is not completely unexpected in the light of the spectroscopic observation that the N7 position of the guanine base appears to be a strong major groove binding site for Mn^{2+} ions (Daune, 1974; Eichhorn, 1981). Transition metals, in general, show a much greater affinity for the nitrogens and oxygens of the heterocyclic bases than do Mg^{2+}, Ca^{2+}, and Ba^{2+} ions. Groove binding, however, further emphasizes the long range nature of the attraction that must extend through several layers of water.

Because temperature-driven associations necessarily imply the presence of an entropy increase, we must ask which of the three species is responsible for this increase. It cannot be the DNA, itself driven from random

solution into an ordered array, nor the $MnCl_2$ whose efficacy is increased by higher bulk concentrations with necessarily lower entropies. Only the water is left. The implication is that there is an entropy increase from the release of structured water during divalent ion binding and/or molecular assembly.

To test this idea of causative entropy increase due to the release of structured water surrounding the helices to the bulk, we replaced $MnCl_2$ with $Mn(ClO_4)_2$ or $MnSO_4$ whose "chaotropic" or "lyotropic" anions, respectively, increase or decrease the entropy of 'bulk' water in the bathing medium. These anions should not closely approach or bind to the negatively charged helices. The idea is that by changing the water entropy of the bath and not of the hydrated DNA, one will modulate from outside the entropy change of water release upon DNA ion binding and assembly. Approximate 'cloudpoint' transition temperatures are shown in Table 1. Anion replacement indeed has a clear effect. Transition temperatures at the same Mn^{2+} concentration are higher in SO_4^{2-} solution than Cl^-, and lower in ClO_4^-. Similar results were reported by Knoll et al. (1988).

Not only is the transition from repulsion to attraction controlled by temperature, but also the apparent magnitude of the net attraction is sensitive to temperature after assembly occurs. Some idea of the range and temperature dependence of attraction is given by the data of Fig. 2, which shows the interaxial spacing versus temperature for DNA arrays formed in 150 mM $Mn(ClO_4)_2$. The distance between surfaces can be as much as 11 Å at 5°C, and this distance significantly decreases with increasing temperature (down to some 8 Å between molecular surfaces at 40°C). The Gaussian width of the interaxial reflection also decreases significantly with increasing temperature, from ~0.8 Å at 5°C to 0.3 Å at 40°C, further showing the strengthening of attraction with increasing temperature.

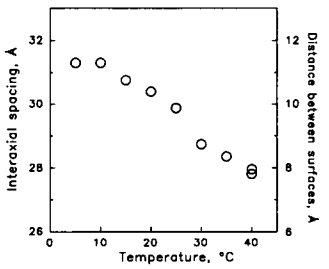

FIGURE 2 The dependence of the equilibrium spacing between DNA helices precipitated in 0.15 M $Mn(ClO_4)_2$, 10 mM Tris, on temperature is shown. Helices move closer as the temperature increases. Changes in spacing are reversible between 5 and 40°C.

Molecular force curves with $MnCl_2$ solution

These qualitative observations from cloudpoint transitions can be verified and quantitated through direct measurement of intermolecular forces by combined osmotic stress and x-ray scattering. This technique has the invaluable capability of connecting structure and phase transitions to thermodynamics through directly observed Π-V work. We proceed by direct force measurement to characterize these long-range, solvent-entropic, temperature-driven, ion-specific interactions that act to assemble these polar molecules.

The observation from 'cloudpoint' transitions in dilute aqueous solution that Mn^{2+} is unlike most other divalent cations in causing precipitation of DNA is readily apparent from molecular force curves. Fig. 3 shows direct force measurements for Mn^{2+}, Ca^{2+}, Zn^{2+}, putrescine at 20°C. Only the Mn^{2+} data shows evidence of a clear transition in spacing at a well defined pressure. As discussed earlier, at spacings wider than the break point, the repulsion between Mn-DNA helices shows about the same decay lengths seen in most uni- and divalent salt solutions at interaxial spacings greater than 30 Å (Rau et al., 1984; Podgornik et al., 1989). At stresses above the transition pressure, however, the force is still exponential but with a decay constant half

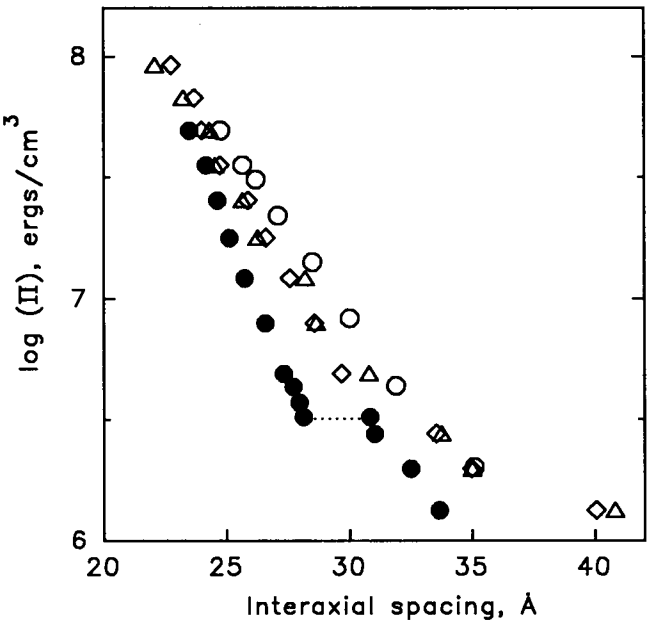

FIGURE 3 A comparison of DNA force curves seen with different divalent ions at 20°C. 10 mM $PutrescineCl_2$, 10 mM Tris (○). 10 mM $ZnCl_2$, 10 mM Tris (△). 10 mM $CaCl_2$, 10 mM Tris (◇). 10 mM $MnCl_2$, 10 mM Tris (●). Only the $MnCl_2$ data shows a clear transition.

the previous value. None of the other divalents shows this type of behavior. Even at very high pressures, there is an apparent 2.5–3.0 Å exponential decay length, with no indication of an abrupt transition.

The bulk $MnCl_2$ concentration dependence of the 'cloudpoint' transition temperature in aqueous solution is apparent in the molecular force curves from the dependence of transition pressures on Mn^{2+} concentration. Fig. 4 shows molecular force curves at 20°C for 5, 10, 25, and 50 mM $MnCl_2$. All show clear breaks in spacing at well defined pressures. Transition osmotic stresses are dependent on bulk $MnCl_2$ concentration, the lower the concentration the higher the critical pressure.

There is a very nearly common curve after the transition. Interhelical forces are independent of Mn concentration at high pressures. The exponential 1.4 ± 0.2 Å decay length is characteristic of forces between DNA helices spontaneously precipitated by multivalent ions, such as cobalt hexammine and spermidine. Before the transition, an exponential decay length of ~3.5 ± 0.5 Å is observed for 10–50 mM $MnCl_2$, and somewhat larger for 5 mM, ~5 Å. These are all significantly smaller and less dependent on ionic strength than expected Debye shielding lengths (7.5–25 Å for the range of $MnCl_2$ concentrations). Unlike any other uni- or divalent counterions we have examined, there is a significant dependence of force amplitude on bulk $MnCl_2$ concentration, an approximate threefold difference between 5 and 50 mM $MnCl_2$ in the 30–40 Å region. A similar dependence of force magnitude on cobalt hexammine concentration was also observed by us in mixed Co^{3+}/Na^+ salt solutions. This dependence, however, is easily rationalized as reflecting changes in cobalt binding in competition with Na^+. The only other counterion present to compete with Mn^{2+} is tris at 10 mM, a very poor competitor for DNA binding. Under the same buffer conditions, neither Mg^{2+} nor putrescine shows a significant dependence of the force magnitude on divalent concentration in this range of interhelical spacings. We will return below to these concentration induced changes applying a generalization of the Clausius-Clapeyron equation to relate changes in Mn activity to changes in the number of Mn ions associated with attraction-causing sites when collapse occurs.

Visually similar relations between force and separation are seen in Fig. 5 when the $MnCl_2$ concentration is fixed (50 mM) and forces are measured at different temperatures (5, 20, 35, and 50°C). Again there is the set of breaks at different collapse pressures, with halving of

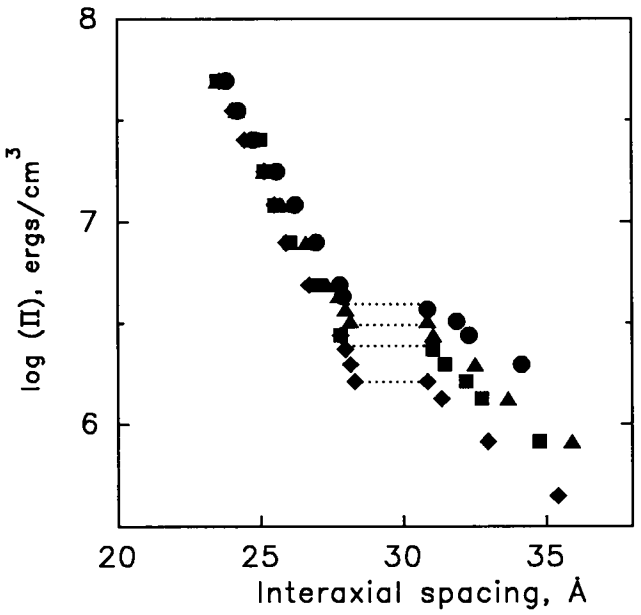

FIGURE 4 The dependence of force curves on $MnCl_2$ concentration at 20°C. 5 mM $MnCl_2$, 10 mM Tris (●). 10 mM $MnCl_2$, 10 mM Tris (▲). 25 mM $MnCl_2$, 10 mM Tris (■). 50 mM $MnCl_2$, 10 mM Tris (◆). Force magnitudes at low osmotic stress and transition pressures for the abrupt change in spacing are dependent on $MnCl_2$ concentration. Force magnitudes at high stress are relatively insensitive to divalent concentration.

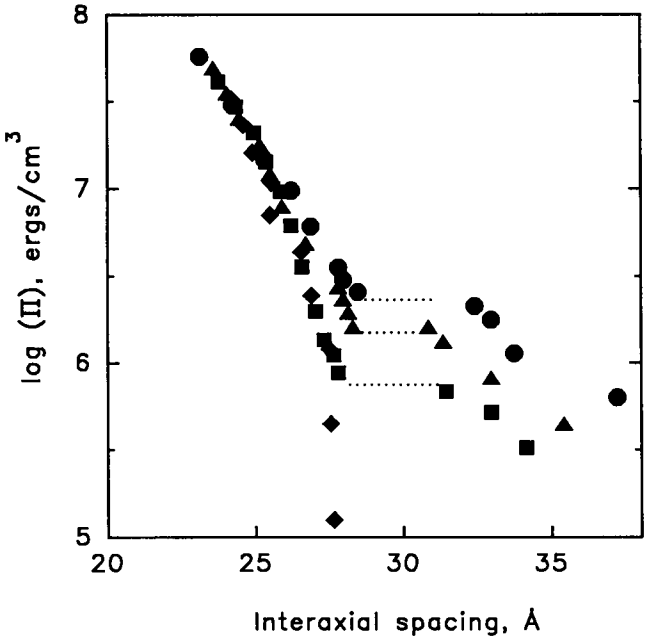

FIGURE 5 The sensitivity of force curves and transitions at constant $MnCl_2$ concentration to temperature. 5°C (●). 20°C (▲). 35°C (■). 50°C (◆). All samples contain 50 mM $MnCl_2$, 10 mM TrisCl. Spontaneous precipitation (no applied osmotic stress) occurs at ~40–45°C. Force magnitudes at low stress and transition pressures decrease with increasing temperature. At high stress, all curves merge.

the ~3–3.5 Å exponential decay rates, characteristic of hydration repulsion, and near merger of all force curves after collapse. Consistent with the observation of a cloud-point at 40–45°C, one observes a finite swelling at 50°C, while progressively greater pressures must be applied to effect collapse at lower temperatures. Once again unlike other counterions we have investigated, there is a strong dependence of the force magnitude on temperature at lower pressures.

Unlike some of the cloud point transitions in aqueous solution, we observe no problems of reversibility in these osmotic stress measurements. DNA pellets readily expand or contract in response to changing osmotic, temperature, or ionic conditions. The measurements reflect equilibria.

Forces with $Mn(ClO_4)_2$

The effect of ClO_4^- on bulk water thermodynamics is sensitive to anion concentration. For most processes affected by anions in the Hofmeister series, a concentration in the tenths molar range is necessary for an observable effect (for a review of Hofmeister effects, see Collins and Washabaugh, 1985). Table 1 shows that the same is true for cloud point transitions of DNA with Mn^{2+}. There is no difference between Cl^- and ClO_4^- with 5 and 10 mM Mn^{2+}, while clear effects are seen at 50 and 150 mM (0.1 and 0.3 M ClO_4^-). Molecular force curves show the same behavior. Fig. 6 compares forces observed in Cl^- or ClO_4^- with 10 and 50 mM Mn^{2+}, at 20°C. At 10 mM, the two curves overlap within experimental error over the entire range of measured spacings. An observable difference between the two anions is apparent at 50 mM. The magnitude of the force at low pressures is decreased in ClO_4^-. The apparent decay length is unaffected. The critical pressure for the transition between force curves is also smaller with ClO_4^- as the anion. After the transition, no difference in force is observed between the two anions.

The temperature dependence of forces in 50 mM $Mn(ClO_4)_2$ is shown in Fig. 7. Replacement of Cl^- by ClO_4^- gives the appearance of simply having raised the temperature. At constant temperature, both low stress force magnitudes and transition pressures are smaller with ClO_4^- than Cl^- at the same concentration. These differences will be examined quantitatively below to relate transition entropies and the solution thermodynamics of these two anions.

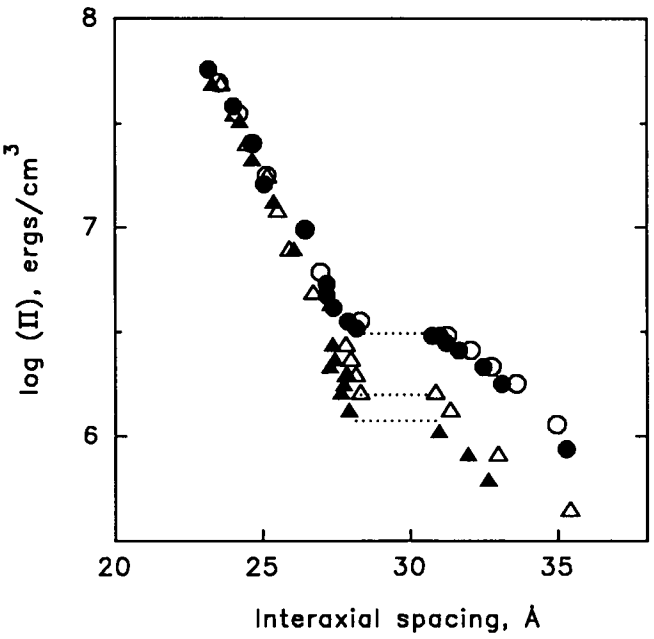

FIGURE 6 Comparison of force curves in $MnCl_2$ and $Mn(ClO_4)_2$ solutions at 20°C. 10 mM $MnCl_2$, 10 mM Tris (○). 10 mM $Mn(ClO_4)_2$, 10 mM Tris (●). 50 mM $MnCl_2$, 10 mM Tris (△). 50 mM $Mn(ClO_4)_2$, 10 mM Tris (▲). No difference in force curves between the two anions in 10 mM Mn^{2+} is observed. At 50 mM Mn^{2+}, however, both force magnitude at low applied stress and transition pressure are smaller in ClO_4^- solution than Cl^-.

DISCUSSION

Strong, specific, entropically favored, long-range attraction between polar moieties can act to assemble macromolecules. We assert that such a generalization is possible from the forces we now have observed between DNA double helices organized into ordered arrays by warming DNA in Mn^{2+} solutions. One is not restricted to think of this "hydrophobic bonding," a thermally inspired drive to organize macromolecules, as a phenomenon of nonpolar materials only. These studies with Mn^{2+} ion reveal a solvent-entropic drive that can be quantified, modified and modulated to give a degree of refinement in forces impossible to achieve by traditional "hydrophobic" bonding. And the ability to control assembly/disassembly by varying the ionic content of the bathing medium introduces new modes of thinking about the importance of the solution environment governing macromolecular organization.

The remarkable range of attraction is obvious in the fact that the molecules assembled do not touch but rather spontaneously assume separations of up to 11 Å between surfaces (using the 20 Å outer diameter of the double helix as a measure of molecular radius).

Attraction strengthens with increasing temperature. Molecules that were sitting at 11 Å separation at 5°C move together to 8 Å to form a tighter lattice at 40°C (Fig. 2).

While we have seen such features of specificity,

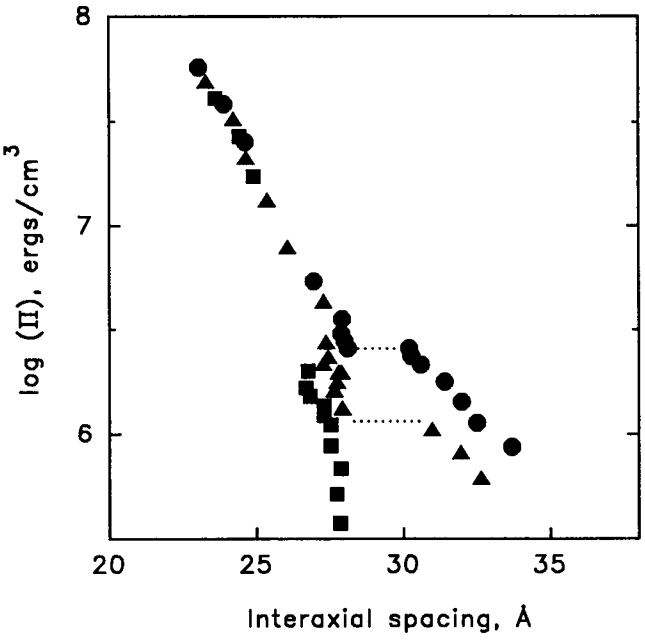

FIGURE 7 Dependence of DNA force curves in 50 mM $Mn(ClO_4)_2$, 10 mM Tris solution on temperature. 5°C (●). 20°C (▲). 35°C (■). Spontaneous precipitation for these ionic conditions occurs at ~30°C.

strength, and control in preparations with other cations, for example, $Co(NH_3)_6^{3+}$ (Rau and Parsegian, 1992), we have not seen the sensitivity of attraction to temperature before. In the experiments reported here, Mn^{2+} is essentially the only counterion present and, as we shall show, there is only a small number of extra ions bound across the transition. Transitions in mixed $Co(NH_3)_6^{3+}/Na^+$ solutions, as we reported earlier, are accompanied by significant changes in $Co(NH_3)_6^{3+}$ binding. The unfavorable entropy from replacing bound Na^+ with trivalent ions would mask the favorable water release entropy observed here.

Among all the divalent cations examined, we have found that only Mn^{2+} and Cd^{2+} confer attractive forces below ~50–60°C. Because assembly is easier with DNA of higher G-C base pair content, it would appear that the action of the cation is "inside" the helix, in the grooves where the base pair composition can be detected (and possibly base stacking slightly modified). DNA binding sites for divalent ions have traditionally been divided into two classes, the phosphates on the backbone and coordination with base oxygens and nitrogens exposed in grooves (Eichhorn, 1973, 1981; Daune, 1974; Saenger, 1984). Alkaline earth metals, such as Mg^{2+} and Ca^{2+}, seem to bind almost exclusively to phosphates, while most transition metals, like Mn^{2+}, can bind to both. Granot et al. (1982a) observed by ^{31}P NMR both inner sphere (direct coordination with loss of bound water) and outer sphere binding of Mn^{2+} to DNA phosphates. There is, additionally, ample evidence for several other binding sites for Mn^{2+} in the helical grooves. The strongest coordination position appears to be the N-7 of purines, particularly guanines, in the major groove (Daune, 1974). Other sites that have been suggested include the O-4 of thymine and the N-3 of purines (Saenger, 1984 and Stevens et al., 1990). Although Granot et al. (1982b) report observing no difference in overall affinity of Mn^{2+} for A-T or G-C rich DNAs by competition, they do infer different modes of binding by NMR.

Just as DNA force amplitudes, but not decay characteristics, in univalent salt solution depend on the particular counterion species bound, so also should force amplitudes in Mn^{2+} solution depend on where the ion is bound. The sensitivity of Mn-DNA force magnitudes to bulk $MnCl_2$ concentration and temperature suggests that relative affinities of Mn^{2+} for the different sites depend on these experimental variables. The sudden transition from repulsion to attraction observed between helices in Mn^{2+} solution may reflect a rearrangement of bound Mn^{2+} among the different sites and a correlation of binding locations on apposing surfaces. We do not, however, understand the differences in binding chemistry sufficiently to explain why Mn^{2+} and Cd^{2+} cause precipitation but not, for example, Ni^{2+} or Zn^{2+}.

Thermodynamic relations

The reversibility and the long-time equilibration of the samples used in our measurements allows us to treat the arrays as thermodynamically well defined phases. We will exploit the possibilities thereby allowed to extract changes in entropy, enthalpy, and ion binding, not just intermolecular force. We will now sketch the thermodynamic relations to be used, then compute entropies of transition and changes in Mn^{2+} binding in several solutions and temperature. In particular, we will point out that the entropy of the solvent and chemical potential of ions in the bathing medium are essential parameters in describing solvent release, entropically favored assembly.

The osmotic stress experiment is thermodynamically equivalent to an experiment in which the DNA containing phase is compressed by a semipermeable piston that exerts a pressure Π equal to the osmotic pressure of the PEG solution. The semipermeable piston membrane allows water and salt, but not DNA, to exchange with a salt solution reservoir (without PEG) of fixed ion and water activities. We assume the activities of the exchanging water and salt are the same in the reservoir and DNA phase and that the exchangeable volume between the DNA phase and the reservoir is due entirely to

water, i.e., the volume of the DNA itself is constant and the volume of exchanging ions is small compared with exchanging water. A complete description of the equivalence of the two experiments is given by Leikin et al. (1991).

The osmotic stress versus interaxial separation relations of Figs. 3–7 are, in fact, thermodynamic relations, measures of the state functions that govern molecular force and assembly. These measurements indicate the change in system free energy dG of the DNA phase with several system variables, specifically osmotic stress Π, temperature T, Mn activity, and (if one thinks a little) percent G-C. To each of these system parameters there is a conjugate variable, DNA phase volume, V, DNA phase entropy, S, number of Mn associated with the DNA phase, n_{Mn}, etc., which can be extracted by elementary considerations.

In another place (Leikin et al., 1991), we have extracted changes in (exponentially growing) entropy, enthalpy, and ion binding as smooth functions of double helix separation. Here we will concentrate on the abrupt pressure, distance discontinuities, that closely resemble first order phase transitions. One may construct a generalization (Prouty et al., 1985) of the Clausius-Clapeyron equation. Specifically, consider the transition between two states. By definition the free energy G of the DNA phase is the same on both sides of the transition for a constant number of DNA molecules,

$$G_1 = G_2. \tag{2}$$

More importantly, this equality is preserved when the phase transition is shifted by a change in system variable x.

$$dG_1/dx = dG_2/dx. \tag{3}$$

The total derivative here signifies the inclusion of all consequences of changing experimental variable x. To be specific, we will consider changes in the experimental variables temperature T and osmotic stress Π, at constant Mn^{2+} activity.

Recalling that,

$$dG = -S\,dT + V\,d\Pi \tag{4}$$

so that

$$dG/d\Pi = -S\,(dT/d\Pi) + V. \tag{5}$$

The derivative is taken both for G_1 and G_2 where the values of T and Π are the experimentally observed transition temperatures T_{tr} and osmotic stresses Π_{tr}.

At a transition pressure, we have,

$$dG_1/d\Pi_{tr} = dG_2/d\Pi_{tr}, \tag{6}$$

which creates the relation

$$-S_1(dT_{tr}/d\Pi_{tr}) + V_1 = -S_2(dT_{tr}/d\Pi_{tr}) + V_2 \tag{7}$$

or the more familiar form, analogous to the Clausius-Clapeyron equation,

$$d\Pi_{tr}/dT_{tr} = -\Delta S/\Delta V. \tag{8}$$

This formalism holds for any two experimental variables, not just temperature and osmotic stress. For example, when one works at constant temperature and sees a change in collapse pressure with different Mn^{2+} chemical potentials, μ_{Mn}, then one has the equation for extracting the change in number of bound or DNA phase associated Mn^{2+} ions, Δn_{Mn},

$$d\Pi_{tr}/d\mu_{Mn} = \Delta n_{Mn}/\Delta V. \tag{9}$$

Changes in Mn ion binding

Fig. 8 shows the dependence of the transition pressure, Π_{tr}, on bulk $MnCl_2$ concentration for 5, 20, and 35°C. At each temperature, the data is well described by a straight line. From Eq. 9, the slope connects the change in the number Mn^{2+} ions bound to DNA and the DNA phase volume change across the transition. At the transition pressure, a change in spacing from D_2 to D_1 corresponds to a volume change per base pair for hexagonally packed B-form DNA of $(\sqrt{3}/2) \times 3.4 \times (D_1^2 - D_2^2)$. The average volume change observed, $\langle \Delta V \rangle$, is ~ 500 Å^3/bp, independent (within about ±20%) of bulk $MnCl_2$ concentration and temperature. The insensitivity of the slopes and volume change to temperature means that the change in number of bound Mn^{2+} across the transition is also about independent of temperature. The extra binding of Mn^{2+} is calculated as 0.01 ions/base pair. In contrast, we previously inferred from the sensitivity of similar transitions to bulk cobalt hexammine concentration that even

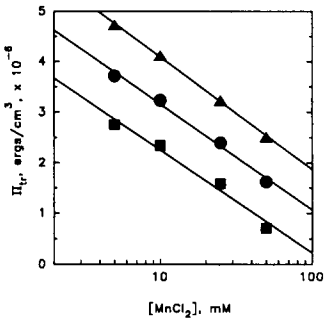

FIGURE 8 Sensitivity of transition pressure to $MnCl_2$ concentration at constant temperature 5°C (▲). 20°C (●). 35°C (■). The slopes of these lines can be related to the number of extra Mn^{2+} ions bound per base pair across transition through Eq. 9.

at the minimum Co^{3+} concentration for spontaneous precipitation of DNA from dilute solution, an extra 0.2 Co^{3+} are bound per base pair. This very small change in binding of Mn^{2+}, in comparison, is consistent with attraction resulting more from a rearrangement of already bound Mn^{2+} among sites rather than additional binding. Results are changed only very slightly if $MnCl_2$ activities rather than concentrations are used. The same difference in number of bound Mn^{2+} across the transition is observed in $Mn(ClO_4)_2$ solutions (data not shown).

Transition entropy changes with Cl^- anion

Plots of transition stress versus temperature are shown in Fig. 9 for the four concentrations of $MnCl_2$ we have examined. The data for each can be well described by a straight line. The extrapolated transition temperature at $\Pi_{tr} = 0$ and 50 mM $MnCl_2$ is ~46°C, in reasonable agreement with the measured cloud point (Table 1). Transition entropy changes calculated from slopes and $\langle \Delta V \rangle = -500$ Å^3/bp are summarized in Table 2. There is very little dependence of the entropy on bulk $MnCl_2$ for concentrations over 10 mM. The entropic contribution ($-T\Delta S$) to the free energy change across the transition is ~ −125 cal/mol base pairs.

Transition entropy changes in ClO_4^- solution

Fig. 10 compares differences in sensitivity of transition temperature to osmotic pressure between Cl^- and ClO_4^- solutions at 10 and 50 mM Mn^{2+}. Water volume changes across the transition are the same for both anions. At 10 mM, there is no observable difference. A clear difference is seen at 50 mM Mn^{2+}. There is a significantly larger entropy of assembly in ClO_4^-. The results are summarized in Table 2. The extra entropic contribution to the transition free energy in replacing Cl^- with ClO_4^- is some −75 cal/mol base pairs.

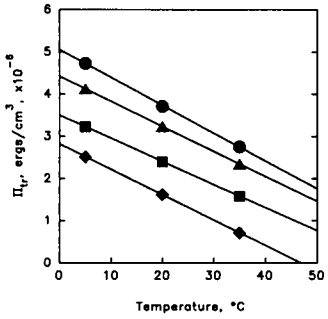

FIGURE 9 Sensitivity of transition pressure to temperature at constant $MnCl_2$ concentration. 5 mM $MnCl_2$, 10 mM Tris (●). 10 mM $MnCl_2$, 10 mM Tris (▲). 25 mM $MnCl_2$, 10 mM Tris (■). 50 mM $MnCl_2$, 10 mM Tris (◆). The slopes of these lines can be related to the entropy change per base pair across the transition through Eq. 8.

TABLE 2 **Entropies of transition**

Salt	ΔS k/base pair	$-T\Delta S$ cal/mol base pairs
(in *mM*)		
5 $MnCl_2$	0.24	−145
10 $MnCl_2$	0.21	−125
25 $MnCl_2$	0.20	−120
50 $MnCl_2$	0.22	−130
10 $Mn(ClO_4)_2$	0.21	−125
50 $Mn(ClO_4)_2$	0.33	−200

Entropy changes calculated from temperature–pressure sensitivities of abrupt transitions in spacing with Eq. 8 and $\langle \Delta V \rangle = 500$ Å^3 for a variety of Mn salt conditions. Values are given for both entropies, in units of the Boltzmann factor (k) per base pair, and the entropic contribution to the free energy, $-T\Delta S$, in cal/mol bp. The error in calculated entropies is ~10%.

Water thermodynamics in Cl^- and ClO_4^- solution

We have already argued that of the three components in solution, the DNA itself, the salt, and the water, the favorable entropy of assembly must come from the

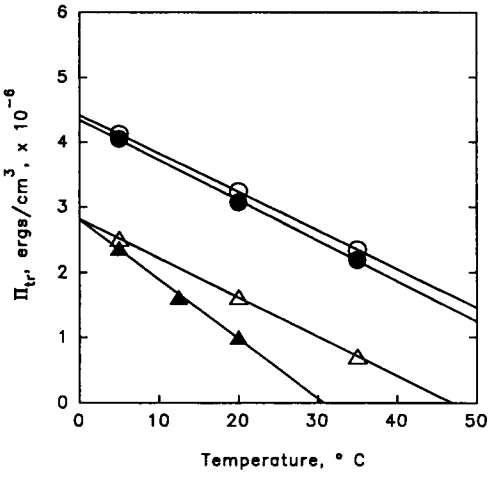

FIGURE 10 Comparison of transition pressure sensitivity to temperature for two concentrations of $MnCl_2$ and $Mn(ClO_4)_2$. 10 mM $MnCl_2$, 10 mM Tris (○). 10 mM $Mn(ClO_4)_2$, 10 mM Tris (●). 50 mM $MnCl_2$, 10 mM Tris (△). 50 mM $Mn(ClO_4)_2$, 10 mM Tris (▲). Differences in slopes of these lines at constant Mn^{2+} concentration between Cl^- and ClO_4^- solution can be related to differences in bulk water thermodynamics.

release of DNA associated, structured water to the bulk solution. It should not be forgotten that the energetics of releasing that water from a macromolecular surface must include the thermodynamic state of the bulk water. In particular, in any entropically driven process one must note the entropy of the water in the bathing medium. For Δn_w mol of water released from the DNA surface or phase to the bulk solution, the entropy change is,

$$\Delta S_{rel} = \Delta n_w \, (\overline{S}_1(\text{bulk}) - \overline{S}_1(\text{DNA})), \tag{10}$$

where $\overline{S}_1$ is a partial molar entropy of water.

Anions in the Hofmeister series affect differently the average enthalpy and entropy of water (Collins and Washabaugh, 1985). "Chaotropic" ions, such as ClO_4^-, are generally considered "water structure breakers," the entropy of water is higher in the presence of ClO_4^- than in solutions of Cl^- anions at the same concentration. If the anion concentration between helices at some 30–35 Å interaxial spacing is negligibly small compared with bulk, then the entropy of water in the DNA phase will be independent of whether the bulk solution contains either Cl^- or ClO_4^-. From Eq. 10, the difference in entropies for transferring water from the DNA phase to a Cl^- solution and from the DNA phase to a ClO_4^- solution is then just the difference in bulk water entropies,

$$\Delta S_{rel}\,(\text{DNA} \rightarrow ClO_4^-) - \Delta S_{rel}\,(\text{DNA} \rightarrow Cl^-) = \Delta n_w \, [\overline{S}_1(ClO_4^-) - \overline{S}_1(Cl^-)]. \tag{11}$$

Water entropies in salt solution are traditionally divided into two components. There is a water entropy from the hydration of ions at infinite dilution (e.g., Friedman and Krishnan, 1973), S_1^0, and also an excess water entropy, S_1^{ex}, that is essentially a correction term for finite salt concentrations to account for ion–ion interactions (e.g., Lewis and Randall, 1961).

For a molal concentration m of MnX_2 (X^- = Cl^- or ClO_4^-), i.e., m moles of salt in 55.6 mol of water, the entropy of hydration per mole of water for 'isolated' ions is,

$$\overline{S}^0_{1,tot} = \frac{m}{55.6} [S_1^0(Mn^{2+}) + 2\,S_1^0(X^-)]. \tag{12}$$

The difference in 'isolated' ion partial molar water entropies between $MnCl_2$ and $Mn(ClO_4)_2$ solutions is simply,

$$\Delta\overline{S}^0_1(Cl^- \rightarrow ClO_4^-) = 2\,m\,[S_1^0(ClO_4^-) - S_1^0(Cl^-)]/55.6. \tag{13}$$

The difference in hydration entropies between Cl^- and ClO_4^- for isolated ions has been estimated by Krestov (1962a,b) as +5.9 cal/mol ion-°K. At 25°C and 50 mM salt concentration, the difference in water entropic energy between $MnCl_2$ and $Mn(ClO_4)_2$ solutions ($-T\Delta\overline{S}^0_1(Cl \rightarrow ClO_4)$) is then ~ -3.2 cal/mol water.

Excess partial molar water entropies at finite salt concentrations can be calculated from excess free energies and enthalpies of water. The partial molar excess free energy of water in MnX_2 salt solution at a molal concentration m is,

$$\overline{G}_1^{ex} = 3RTm\,(1 - \phi)/55.6, \tag{14}$$

where ϕ is the osmotic coefficient, which is dependent on salt concentration and ionic species.

Partial molar excess enthalpies of water are calculated from relative apparent molar heat contents, ϕ_L. For a molal concentration m, the excess water enthalpy is,

$$\overline{H}^{ex} = -\frac{m}{55.6}\frac{\partial\phi_L}{\partial m}. \tag{15}$$

The partial molar excess entropic contribution of water to the free energy is then,

$$-T\,\overline{S}_1^{ex} = \overline{G}_1^{ex} - \overline{H}_1^{ex}. \tag{16}$$

Osmotic coefficients at 25°C for both $MnCl_2$ and $Mn(ClO_4)_2$ solutions are tabulated by Goldberg (1979). Relative apparent heat contents at 25°C are given in Goldberg (1979) for $MnCl_2$ and in Gier and Vanderzee (1974) for $Mn(ClO_4)_2$. From these data, we calculate that in 50 mM Mn^{2+} the difference in excess entropic energy of water, $-T\Delta\overline{S}_1^{ex}$ between ClO_4^- and Cl^- solutions is only -0.2 cal/mol water.

Combining the partial molar water entropies from both isolated ion and excess contributions, the entropic energy differences between $Mn(ClO_4)_2$ and $MnCl_2$ bulk solutions at 50 mM salt for the release of 1 mol water is -3.4 cal.

The observed difference in transition entropic energies between Cl^- and ClO_4^- solutions is some -75 cal/mol base pair. How much of this difference can be explained by bulk water entropy differences? The 500 $Å^3$ volume change per base pair is almost entirely from exchanging water and corresponds to ~ 17 mol water released per mole base pair. The expected energy difference due solely to bulk water effects is ~ -60 cal/mol base pair. The difference in bulk water entropies can virtually account for all the entropy difference in the transition we observe.

We cannot conclusively distinquish between an attraction caused by direct electrostatic attraction between correlated charges on apposing surfaces with a constant dielectric medium and an attraction between correlated charges on apposing surfaces mediated by water structuring. Our observations of exponentially varying forces with very characteristic decay lengths for a variety of

materials and now our observation of the sensitivity of attraction to bulk water entropies, however, argue that water structuring must play at least an important, if not dominant, role.

CONCLUSIONS

The power of polar surfaces to immobilize or to organize water is, in our opinion, still a neglected feature of forces driving the organization of soluble macromolecules. By now, the virtual ubiquity of dominant hydration forces in the last 1 or 2 nm of separation is well established (Parsegian et al., 1987; Rand and Parsegian, 1989). Between soluble molecules, the force is usually necessarily repulsive as surfaces cling to solvent. But attractive hydration forces have now appeared. The temperature dependence of the attractive forces described in this work suggests that much of what had been traditionally put down to "hydrophobic" interactions between nonpolar moieties (Franks, 1975) could in fact be due to the attraction of polar surfaces.

The comparatively rich possibilities of arranging polar surfaces allows one to see how chemical modification or ion binding can change repulsion to attraction and can solve a fundamental paradox in molecular assembly. How do molecular components stay soluble then bond strongly to the right mate? High energy non polar surfaces are insoluble and precipitate at first opportunity. Polar surfaces also of high energy have the faculty to repel by solvation and to attract with similar affinity when the match is right. The strength of the attractive forces we have seen creating DNA arrays is 50 to 100 times as strong as the van der Waals force that is the usual candidate for attraction (Rau and Parsegian, 1992). The sensitivity of attractive forces to small changes in ionic, solvent, or osmotic environment opens up essential possibilities of reversibility and control. The thermal and osmotic sensitivity of the forces described here combined with similar features of protein assembly (Prouty et al., 1985) or protein rearrangement (Zimmerberg and Parsegian, 1986) should provide a better vocabulary for molecular organization than has been available until now.

Received for publication 3 May 1991 and in final form 26 July 1991.

REFERENCES

Collins, K. D., and M. W. Washabaugh. 1985. The Hofmeister effect and the behavior of water at interfaces. *Quart. Rev. Biophys.* 18:323–422.

Daune, M. 1974. Interactions of metal ions with nucleic acids. *In* Metal Ions in Biological Systems, Vol. 3, High Molecular Weight Complexes. H. Sigel, editor. Marcel Dekker, New York. 1–43.

Eichhorn, G. L. 1973. Complexes of polynucleotides and nucleic acids. *In* Inorganic Biochemistry, Vol. 2. G. L. Eichhorn, editor. Elsevier, New York. 1210–1243.

Eichhorn, G. L. 1981. The effect of metal ions on the structure and function of nucleic acids. *Adv. Inorgan. Biochem.* 3:1–46.

Eichhorn, G. L., and Y. A. Shin. 1969. Interaction of metal ions with polynucleotides and related compounds. XII. The relative effect of various metal ions on DNA helicity. *J. Am. Chem. Soc.* 90:7323–7328.

Franks, F. 1975. The hydrophobic interaction. *In* Water: A Comprehensive Treatise, Vol. 4. F. Frank, editor. Plenum Press, New York. 1–94.

Friedman, H. L., and C. V. Krishnan. 1973. Thermodynamics of ion hydration. *In* Water: A Comprehensive Treatise, Vol. 3. F. Frank, editor. Plenum Press, New York. 1–118.

Gier, L. J., and C. E. Vanderzee. 1974. Enthalpies of dilution and relative apparent molar enthalpies of aqueous calcium and manganese perchlorate. *J. Chem. Eng. Data.* 19:323–325.

Goldberg, R. N. 1979. Evaluated activity and osmotic coefficients for aqueous solutions: bi-univalent compounds of lead, copper, manganese, and uranium. *J. Phys. Chem. Ref. Data.* 8:1005–1050.

Granot, J. H., J. Feigon, and D. R. Kearns. 1982a. Interactions of DNA with divalent metal ions. I. ^{31}P-NMR studies. *Biopolymers.* 21:181–201.

Granot, J. H., N. Assa-Munt, and D. R. Kearns. 1982b. Interactions of DNA with divalent metal ions. IV. Competitive studies of Mn^{2+} binding to AT- and GC-rich DNAs. *Biopolymers.* 21:873–883.

Knoll, D. A., M. G. Fried, and V. A. Bloomfield. 1988. Heat-induced DNA aggregation in the presence of divalent metal salts. *In* Structure & Expression, Vol. 2: DNA and Its Drug Complexes. R. H. Sarma and M. H. Sarma, editors. Adenine Press, New York. 123–145.

Krestov, G. A. 1962a. The thermodynamic characteristics of structural changes in water accompanying the hydration of ions. *J. Struct. Chem.* 3:125–130.

Krestov, G. A. 1962b. The thermodynamic characteristics of structural changes in water connected with the hydration of polyatomic and complex ions. *J. Struc. Chem.* 3:391–398.

Leikin, S., D. C. Rau, and V. A. Parsegian. 1991. Measured entropy and enthalpy of hydration as a function of distance between DNA double helices. *Phys. Rev. A.* 44:5272–5278.

Lewis, G. N., and M. Randall. 1961. Thermodynamics. Revised by K. S. Pitzer and L. Brewer. McGraw-Hill, New York. 373–403.

McGhee, J. D., W. I. Wood, M. Dolan, J. D. Engel, and G. Felsenfeld. 1981. A 200 base pair region at the 5′ end of the chicken adult β-globin gene is accessible to nuclease digestion. *Cell.* 27:45–55.

Michel, B. E. 1983. Evaluation of the water potentials of solutions of polyethylene glycol 8000 both in the absence and presence of other solutes. *Plant Physiol.* 72:66–70.

Mudd, C. P., H. Tipton, V. A. Parsegian, and D. C. Rau. 1987. Temperature-controlled vacuum chamber for x-ray diffraction studies. *Rev. Sci. Instrum.* 58:2110–2114.

Parsegian, V. A., R. P. Rand, N. L. Fuller, and D. C. Rau. 1986. Osmotic stress for the direct measurement of intermolecular forces. *Methods Enzymol.* 127:400–416.

Parsegian, V. A., R. P. Rand, and D. C. Rau. 1987. Lessons from the direct measurement of forces between biomolecules. *In* Physics of

Complex and Supermolecular Fluids. S. A. Safran and N. A. Clark, editors. John Wiley and Sons, New York. 115–135.

Podgornik, R., and V. A. Parsegian. 1990. Molecular fluctuations in the packing of polymeric liquid crystals. *Macromol.* 23:2265–2269.

Podgornik, R., D. C. Rau, and V. A. Parsegian. 1989. The action of interhelical forces on the organization of DNA double helices: fluctuation-enhanced decay of electrostatic double-layer and hydration forces. *Macromol.* 22:1780–1786.

Prouty, M. S., A. N. Schechter, and V. A. Parsegian. 1985. Chemical potential measurements of deoxyhemoglobin S polymerization: determination of the phase diagram of an assembling protein. *J. Mol. Biol.* 184:517–528.

Rand, R. P. 1981. Interacting phospholipid bilayers: measured forces and induced structural changes. *Annu. Rev. Biophys. Bioeng.* 10:277–314.

Rand, R. P., and V. A. Parsegian. 1989. Hydration forces between phospholipid bilayers. *Biophys. Biochem. Acta.* 988:351–376.

Rau, D. C., B. Lee, and V. A. Parsegian. 1984. Measurement of the repulsive force between polyelectrolyte molcules in ionic solution: hydration forces between parallel DNA double helices. *Proc. Natl. Acad. Sci. USA.* 81:2621–2625.

Rau, D. C., and V. A. Parsegian. 1990. Direct measurement of forces between linear polysaccharides xanthan and schizophyllan. *Science (Wash. DC).* 249:1278–1281.

Ray, D. C., and V. A. Parsegian. 1992. Direct measurement of the intermolecular forces between counterion condensed DNA double helices. *Biophys. J.* 61:246–259.

Saenger, W. 1984. Principles of Nucleic Acid Structure. Springer-Verlag, New York. 201–219.

Stevens, J. M., H. Oberoi, and I. M. Russu. 1990. A nuclear magnetic resonance study of Mn^{++} ions with DNA. *Biophys. J.* 57:448a. (Abstr.)

Zimmerberg, J., and V. A. Parsegian. 1986. Polymer inaccesible volume changes during opening and closing of a voltage-dependent ionic channel. *Nature (Lond.).* 323:36–39.